Cell, Vol. 119, 503–516, November 12, 2004, Copyright ©2004 by Cell Press

Mammalian Pins Is a Conformational Switch that Links NuMA to Heterotrimeric G Proteins

Quansheng Du and Ian G. Macara*
Center for Cell Signaling
Department of Microbiology
University of Virginia School of Medicine
Charlottesville, Virginia 22908

Summary

During asymmetric cell divisions, mitotic spindles align along the axis of polarization. In invertebrates, spindle positioning requires Pins or related proteins and a G protein α subunit. A mammalian Pins, called LGN, binds Gαi and also interacts through an N-terminal domain with the microtubule binding protein NuMA. During mitosis, LGN recruits NuMA to the cell cortex, while cortical association of LGN itself requires the C-terminal Gα binding domain. Using a FRET biosensor, we find that LGN behaves as a conformational switch: in its closed state, the N and C termini interact, but NuMA or Gαi can disrupt this association, allowing LGN to interact simultaneously with both proteins, resulting in their cortical localization. Overexpression of Gαi or YFP-LGN causes a pronounced oscillation of metaphase spindles, and NuMA binding to LGN is required for these spindle movements. We propose that a related switch mechanism might operate in asymmetric cell divisions in the fly and nematode.

Introduction

During mitosis, microtubules (MTs) reorganize into bipolar spindles that attach the chromosomes to the centrosomes and also into asters that radiate from the spindle poles and attach the centrosomes to the cell cortex (Compton, 2000). The spindles exert tension on the sister chromatids and drive chromatid separation during anaphase. The asters determine the position and orientation of the centrosomes. During asymmetric cell divisions, polarization drives fate determinants to one end of the cell, and the centrosomes then orient so that, after mitosis, the determinants are segregated to only one of the two daughters (Doe and Bowerman, 2001; Jan and Jan, 2001; Macara, 2004). Spindle orientation is also important during morphogenesis, for instance, in the formation of epithelial sheets, where cells must divide within the plane of the sheet (Reinsch and Karsenti, 1994). In the asymmetric cell divisions of *Drosophila* neuroblasts and in sensory organ precursor cells, the positioning of the spindle has been shown to require a protein called Pins and the Gα subunit of a heterotrimeric G protein (Schaefer et al., 2000, 2001; Yu et al., 2000). Pins localizes to one end of the cell and binds to Gα, which is attached to the plasma membrane through an N-terminal myristoyl group. GoLoco motifs present in the C-terminal half of Pins bind to Gα in its GDP bound state (Willard et al., 2004). In the absence of either protein, spindle orientation is randomized. Gene products related to Pins—GPR 1,2—and to Gα—GOA-1/GPA16—are also essential for spindle positioning in the *C. elegans* zygote (Gotta and Ahringer, 2001; Gotta et al., 2003; Colombo et al., 2003; Srinivasan et al., 2003). One hypothesis consistent with these data is that Gα functions in a signaling pathway downstream of Pins to control spindle orientation (Colombo et al., 2003; Schaefer et al., 2001; Schaefer et al., 2000; Willard et al., 2004). The mechanism for orientation is unclear but requires aster attachment to the cell cortex. The aster MTs exert tension on the centrosomes, possibly through the minus end-directed motor protein, dynein (Schneider and Bowerman, 2003). If the cortical dynein is unable to move, it will pull on the asters. Unequal pulling forces will generate torque and/or a translational force on the mitotic apparatus (Grill et al., 2001, 2003).

Examples of asymmetric cell divisions in mammals are rare and are not easily studied at a molecular level (Cayouette and Raff, 2002). Nonetheless, two mammalian proteins related to Pins exist, called LGN and AGS3, and it is tempting to speculate that one or both of these proteins possess a conserved function with other Pins homologs. Mouse LGN can in fact functionally replace Pins in *Drosophila* (Yu et al., 2003). LGN and AGS3 bind specifically to the Gαi and Gαo isoforms of the heterotrimeric G proteins (Willard et al., 2004). The N-terminal half of Pins and its relatives contain tetratricopeptide repeats (TPR) that are commonly involved in protein-protein interactions. The *Drosophila* Pins N terminus binds to Inscuteable (Insc), which in neuroblasts links Pins to a polarity protein called Par-3, but there are no known homologs of Insc in other organisms (Schaefer et al., 2000; Yu et al., 2000).

We identified a nuclear protein, NuMA, as a mammalian binding partner for LGN. NuMA is a large coiled-coil protein that localizes to and organizes the spindle poles (Gaglio et al., 1995; Gordon et al., 2001). The C terminus contains a MT binding domain (Du et al., 2002; Haren and Merdes, 2002). The LGN binding region of NuMA partially overlaps this domain, so NuMA cannot bind LGN and MTs simultaneously (Du et al., 2002). The association of NuMA with MTs is presumably essential for spindle pole organization, because high-level expression of LGN disrupts spindle organization and causes mitotic catastrophe. Moreover, in frog egg extracts, the NuMA binding domain of LGN inhibits the organization of MTs into asters. Depletion of LGN by RNA interference also causes defects in the formation of bipolar spindles in mitotic HeLa cells (Du et al., 2001). These dramatic effects on the mitotic apparatus have made it difficult to determine whether this Pins homolog has additional function in spindle orientation. Nonetheless, LGN has been reported to localize to the cell cortex during mitosis, which is reminiscent of the cortical localization of the *Drosophila* and *C. elegans* Pins proteins (Kaushik et al., 2003).

We now show that Gαi recruits LGN to the cell cortex, that LGN can simultaneously bind to both Gαi and NuMA, and that a small fraction of NuMA is also recruited

*Correspondence: igm9c@virginia.edu

to the cortex during mitosis. Unexpectedly, NuMA association with LGN is necessary for the association of LGN with the cell cortex. Using a FRET biosensor, we found that the N- and C-terminal halves of LGN bind to one another to form a closed state that has a low affinity for Gα and NuMA. On disassembly of the nuclear envelope, NuMA is released into the cytoplasm where it can bind LGN and switch it to an open state, which permits binding to Gαi:GDP at the cell cortex.

Interestingly, overexpression of Gαi induces a pronounced oscillation of the mitotic spindle during metaphase. A similar motion has been observed in dividing embryonic rat neuroepithelial cells (Adams, 1996). The effect is specific for Gαi and is not induced by a GTP bound mutant of the protein. Low-level expression of a YFP-LGN fusion also causes spindle rocking, which requires both NuMA and Gαi binding to LGN. We suggest that the trimeric NuMA/LGN/Gα complex regulates the interaction of aster MTs with the cell cortex and that increased cortical localization of the complex might produce transient imbalances in the pulling forces on the mitotic apparatus, causing them to rock back and forth. This type of conformational switch mechanism is likely conserved among all Pins homologs.

Results

Cell Cycle-Dependent Changes in LGN Localization

Consistent with LGN having an important role in mitosis, the level of expression of the protein varies through the cell cycle, with a peak during M phase that parallels expression of cyclin B1 (Figure 1A). This protein expression pattern is in agreement with the results of a recent cDNA microarray screen, which identified LGN as one of the top 50 genes that are expressed periodically during the HeLa cell cycle (Whitfield et al., 2002). Coincident with this increase in LGN level, the protein becomes localized both to the spindle poles and to the cell cortex, as detected by immunofluorescence (Figure 1B). In interphase cells, this anti-LGN antibody stains speckles scattered throughout the cytoplasm (neighboring cells in Figure 1B).

To validate the antibody staining and to determine which domains of LGN are responsible for its differential localization during mitosis versus interphase, we created inducible stable MDCK cell lines that express YFP-tagged full-length LGN(1-677) or the N-terminal region of LGN (residues 1–373) or the C terminus LGN(358-677). When the YFP-LGN(1–677) fusion protein is expressed at relatively low levels (about 5 × endogenous), the protein is diffuse throughout the cell in interphase, but, consistent with the antibody staining, it becomes concentrated at the cell cortex and spindle poles during mitosis (Figure 1C, and see Supplemental Figure S1 at http://www.cell.com/cgi/content/full/119/4/503/DC1/). Distinct domains in LGN determine these two locations. The N-terminal half of LGN, which contains the TPR repeats and binds NuMA, localizes exclusively to the spindle poles, while the C-terminal half, which contains the GoLoco motifs and binds Gαi, localizes to the cell cortex (Figure 1C). Consistent with previous data (Kaushik et al., 2003), cortical association of LGN is independent of microtubule integrity, whereas association with the spindle poles is abolished when the cells are treated with nocodazole to disassemble microtubules (Supplemental Figure S1). At high expression levels, the YFP-LGN disrupts the attachment of the spindle microtubules to the poles, resulting in mitotic arrest and chromosome missegregation, as we had shown previously for myc-LGN (Supplemental Figure S2) (Du et al., 2001). Interestingly, in mitotic cells expressing YFP-LGN, we observed that endogenous NuMA colocalizes with YFP-LGN not only at spindle poles but also at the cell cortex. However, this cortical NuMA localization was not seen in cells expressing the isolated N-terminal or C-terminal half of LGN (Figure 1C).

The inducible stable cell lines enabled us to monitor YFP-LGN in live cells. The expression of YFP-LGN at moderate levels (<20-fold × endogenous) had no effect on the formation of bipolar spindles (see Supplemental Figure S1 on the *Cell* web site). Moreover, the cells entered anaphase normally and completed cytokinesis after telophase, at which time YFP-LGN dissociated from the spindle poles and the cell cortex (Figure 1D and Supplemental Movie S1).

LGN Recruits NuMA to the Cell Cortex in Mitosis

Previous reports have described NuMA as being nuclear during interphase and exclusively in the spindle pole region during mitosis (Compton et al., 1992). However, we could reproducibly detect a small amount of NuMA staining at the cell cortex of mitotic MDCK cells when using higher concentrations of anti-NuMA antibody, and this distribution was increased by about 5-fold in cells that express YFP-LGN, suggesting that NuMA can be recruited to the cortex by LGN (Figures 1C and 2A). Importantly, as mentioned above, the isolated N terminus and the C terminus of LGN inhibit NuMA recruitment to the cell cortex (Figure 1C).

To determine whether this distribution of NuMA might be an artifact of the antibody staining, we transfected cells with YFP-NuMA and were able to observe YFP fluorescence at the cortex of mitotic cells but not in interphase cells (Figure 2B). A similar result was obtained with RFP-NuMA (data not shown). These data confirm that a small fraction of NuMA localizes to the cell cortex in mitotis.

To definitively test the hypothesis that cortical NuMA is recruited by LGN, we used RNA interference to reduce the endogenous LGN level in HeLa cells. As we have shown previously, loss of LGN causes severe chromosome missegregation in these cells (Du et al., 2001), but, additionally, we observed that cortical NuMA was absent in mitotic cells that had been transfected with LGN-directed siRNA (Figure 2C). We conclude from these data that the cortical localization of NuMA is mediated by LGN binding.

Cobinding of NuMA and Gαi to LGN

The cortical localization of LGN requires its C-terminal GoLoco motifs, which can bind to membrane-associated Gαi. To determine whether Gα is required for cortical localization of LGN and NuMA, we first asked if LGN can bind simultaneously to NuMA and Gαi. We cotransfected COS-7 cells with HA-LGN and/or the HA-tagged C-terminal domain of NuMA (which binds LGN) together

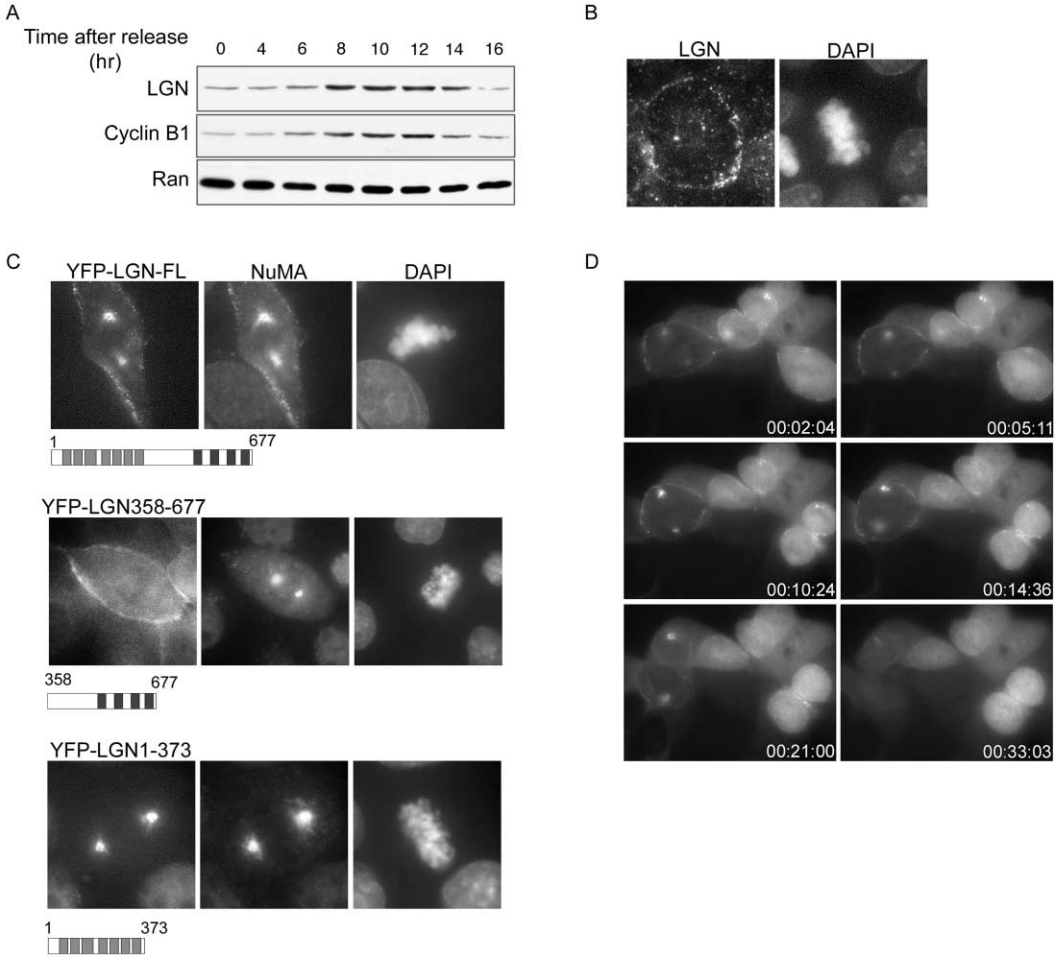

Figure 1. Cell Cycle-Regulated Expression and Localization of LGN

(A) HeLa cells were synchronized by double thymidine (2 mg ml^{-1}) block. At indicated time points after releasing from the block, cells were harvested, and endogenous LGN and cyclin B1 protein were detected by Western blotting. Anti-Ran was used as a control for equal loading.

(B) Immunofluorescence images of MDCK cells using anti-LGN antibodies. DNA was stained with DAPI.

(C) Fluorescence images of MDCK cells stably expressing YFP-fused LGN (1–677, upper panel), LGN (358–677, middle panel), and LGN (1–373, lower panel). Cells were incubated in doxycycline-free medium for 24 hr and subjected to immunostaining with anti-NuMA antibodies. DNA was stained with DAPI. Schematics under each panel show the domain structure of LGN and LGN fragments expressed in the stable cell lines. 100% of the cells examined (>50) showed similar distributions.

(D) Selected frames from a representative time-lapse experiment showing localization of YFP-LGN at different times (indicated at the lower corner of each image as minutes:seconds) during mitosis.

with myc-tagged Gαi1. After immunoprecipitation of the Gαi1 with anti-myc antibody, the NuMA fragment was found to have coprecipitated only when HA-LGN was present (Figure 2D). This result shows that LGN can link Gαi1 to NuMA. To confirm that this ternary interaction is direct, we attached recombinant S-tagged NuMA(1818–2001) to beads and incubated them with purified His6-tagged Gαi1 and/or LGN-His6 or the isolated N terminus of LGN, GST-LGN(1–373). The Gαi1 was bound specifically to the NuMA beads only in the presence of full-length LGN (Figure 2E). As expected, the isolated N terminus of LGN could bind NuMA but not Gαi1. Together, these data show that LGN can bind simultaneously to both NuMA and Gαi1.

Gα Recruits LGN and NuMA to the Cell Cortex

We next transfected cells with a Gαi1-YFP construct. This construct localizes, like the endogenous protein, to the plasma membrane. In these cells, endogenous LGN staining appeared more intense, and was present at the cell cortex, not only in mitotic cells but also in interphase cells (Figure 3A). Moreover, in Gαi-YFP mitotic cells, endogenous NuMA staining at the cortex was more intense than in control mitotic cells (Figure 3B). Quantification of the fluorescence intensity at the cell cortex indicated a 4- to 5-fold increase in membrane association of the LGN and NuMA. Conversely, we did not detect any Gαi-YFP colocalizing with NuMA at the spindle poles. Similar results were obtained using untagged Gαi that was expressed together with YFP as a transfection marker (Supplemental Figure S3B).

LGN binds preferentially to the GDP bound state of Gαi (Natochin et al., 2001). We therefore tested Gαi (Q204L), which is a mutant that is predominantly GTP bound, and found that it did not efficiently recruit LGN to the cell cortex (Supplemental Figure S3C). To confirm

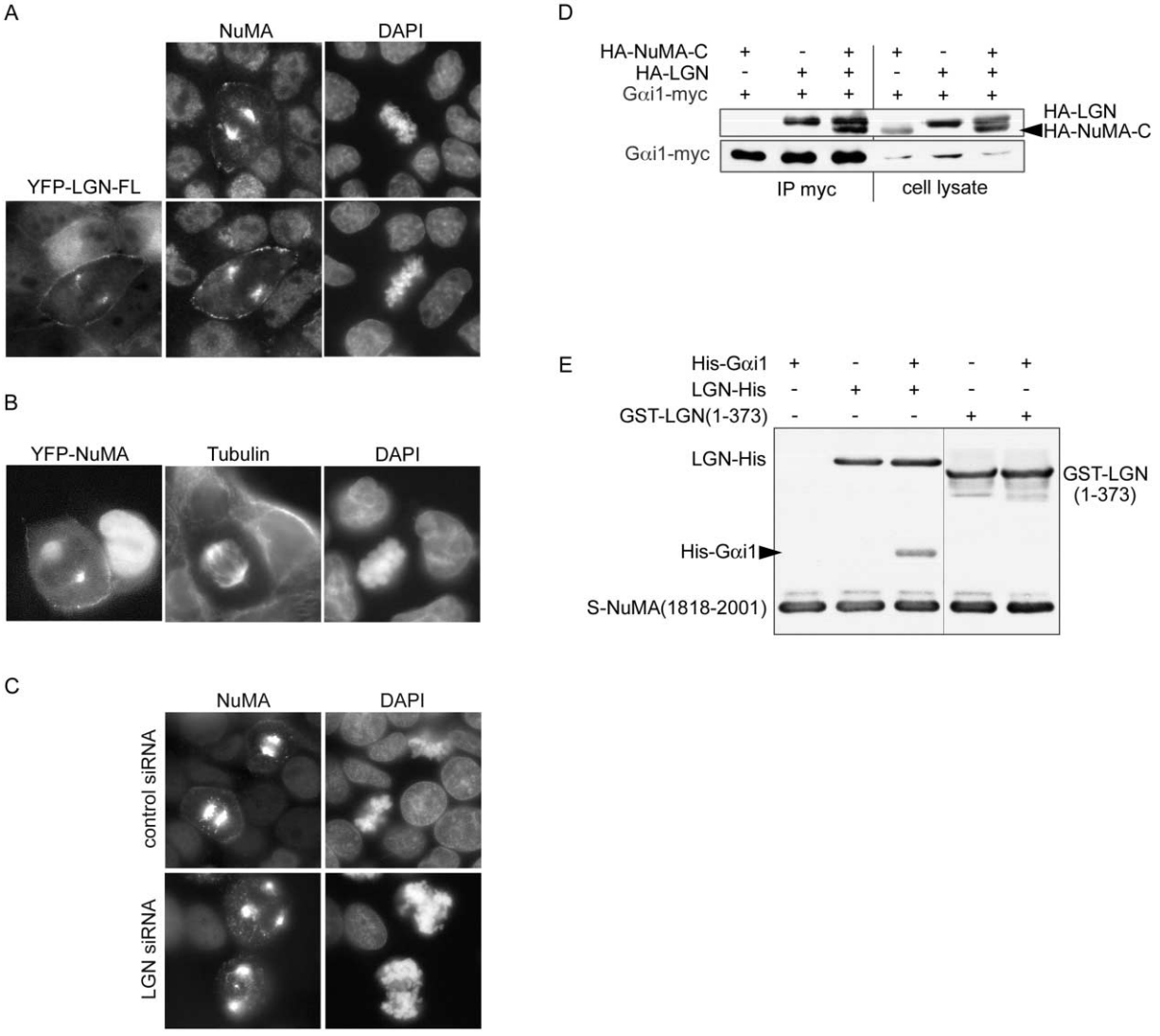

Figure 2. LGN Recruits NuMA to the Cell Cortex and Forms a Complex with Gα

(A) Control (upper panel) and YFP-LGN-expressing (lower panels) MDCK cells were stained with equal amounts of anti-NuMA antibodies, and the images were taken with identical exposure times. DNA was stained with DAPI. Cortical fluorescent intensities were measured for 40 control or YFP-LGN-expressing cells.

(B) Localization of YFP-NuMA in mitotic and interphase MDCK cells. Cells were transfected with pKYFP-NuMA and fixed 24 hr after transfection. Microtubules were stained with anti-tubulin antibody and Alexa 594-conjugated secondary antibodies.

(C) Knockdown of LGN results in the dislocalization of NuMA from the cell cortex. HeLa cells were transfected with a control siRNA or a siRNA targeted against LGN. Images are representative of 25 transfected mitotic cells. Three days posttransfection, the cells were fixed and stained for NuMA and DNA.

(D) Gαi1, LGN, and NuMA-C fragments can form a ternary complex when coexpressed in COS-7 cells. Different combinations of pKGαi1-myc, pKH3-LGN, and pKH3-NuMA-C were transfected into COS-7 cells. Cell lysates were harvested 36 hr posttransfection and immunoprecipitated with 9E10 anti-myc antibody and GammaBind Plus Sepharose beads. Bound proteins were separated by SDS-PAGE and blotted using anti-myc and anti-HA antibodies. One thirtieth of each lysate was also separated and blotted as control.

(E) LGN can bind directly to both Gαi1 and NuMA in vitro. S-tagged NuMA (1818–2001) (2 μg) was loaded on S-agarose beads and incubated with His6-Gαi1 (2 μg, lane 1), LGN-His6 (2 μg, lane 2), GST-LGN(1–373) (2 μg, lane 4), LGN-His6 plus His6-Gαi1 (lane 3), or GST-LGN(1–373) plus His6-Gαi1 (lane 5). Bound proteins were separated by SDS-PAGE and blotted using anti-His6 or anti-GST antibodies.

specificity, we also tested Gαs-GFP, which does not bind LGN (Natochin et al., 2001). Although this G protein was localized to the plasma membrane, no increase in cortical LGN was detectable (Supplemental Figure S3C). Moreover, the recruitment of LGN to the cell cortex during mitosis was prevented by the expression of an RFP-Gαi fusion protein, which is mistargeted to the cytoplasm (Supplemental Figure S3A). Together, these results demonstrate that GDP bound Gαi1 at the plasma membrane can bind to LGN and, through LGN, to NuMA.

To confirm that such a ternary complex can form, cells were transfected with Gαi-myc and harvested for

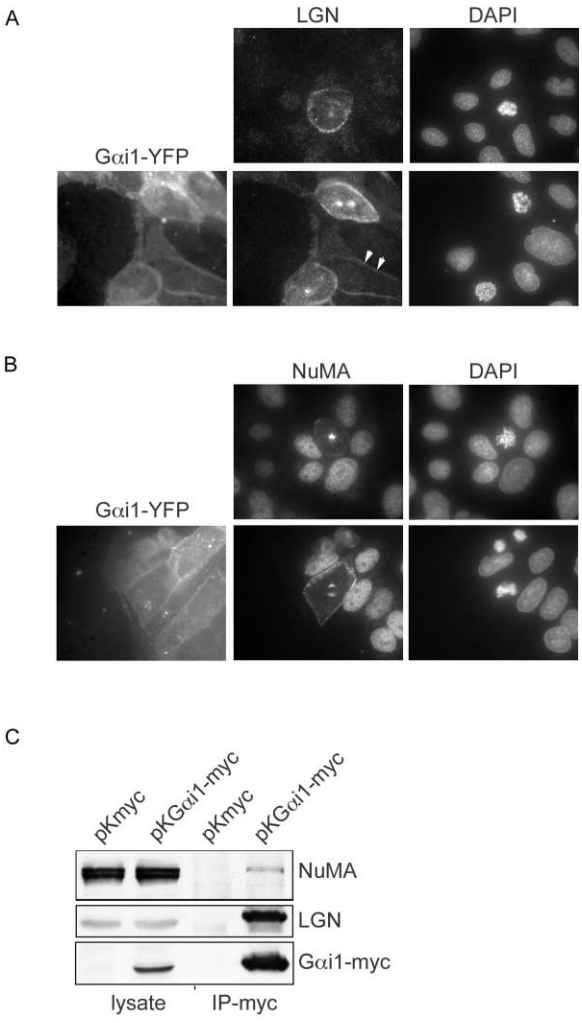

Figure 3. Expression of Gαi1-YFP Increases Cortical Localization of LGN and NuMA

(A and B) Control (upper panels) and pKGαi1-YFP-transfected (lower panels) MDCK cells were fixed and stained with anti-LGN (A) or anti-NuMA (B) antibodies. Images of LGN or NuMA staining were taken with identical exposure times. Cortical fluorescent intensities were measured for 50 control or Gαi1-YFP-expressing cells. DNA was stained with DAPI.

(C) Gαi1-myc can coimmunoprecipitate endogenous LGN and NuMA. HeLa cells were transfected with pKGαi1-myc or pKmyc. Cell lysates were harvested 24 hr posttransfection and immunoprecipitated with 9E10 anti-myc antibody and GammaBind Plus Sepharose beads. Bound proteins were separated by SDS-PAGE and blotted using anti-myc, anti-LGN, or anti-NuMA antibodies. One twentieth of each lysate was also separated and blotted as a control.

immunoprecipitation. Endogenous LGN and a small fraction of the endogenous NuMA were both coprecipitated with the Gαi (Figure 3C).

Intramolecular Self-Interaction of LGN

Why is LGN normally found at the cell cortex only during mitosis? One hypothesis is that LGN is posttranslationally modified such that it can only interact with Gαi during mitosis. However, this explanation is unlikely, since the overexpression of Gαi leads to a recruitment of LGN to the cell cortex even in interphase cells. An alternative hypothesis is that NuMA, which is released from the nucleus at the start of mitosis, alters the conformation of LGN so as to increase its affinity for Gαi, thereby facilitating the association of both proteins to the cortex. This hypothesis suggests that LGN behaves as a switch, with a closed and open conformational state, controlled by NuMA.

In support of this switch mechanism, our initial yeast two-hybrid screen for LGN binding partners identified the C terminus of LGN itself, in addition to NuMA (Du et al., 2001). Multiple independent clones of LGN were isolated from two libraries. The two-hybrid interaction is shown in Figure 4A. Interestingly, this head-tail interaction is conserved: the N- and C-terminal regions of another mammalian Pins homolog, AGS3, also associate with one another (data not shown), as do the domains of the *Drosophila* Pins itself (Figure 4B). The C terminus of Pins also binds to mammalian LGN (1–373), despite the fact that the amino acid identity between this region of LGN and Pins is quite low (32%). And, unexpectedly, *Drosophila* Pins even binds to human NuMA (Figure 4B), a protein with no known *Drosophila* homolog. As a negative control, neither Pins nor LGN interacted with stathmin in this assay.

We next mapped the interaction domains on the N-terminal and C-terminal halves of LGN by yeast two-hybrid and in vitro binding assays. The N-terminal TPR motifs 1 and 2 of LGN, which also bind NuMA, are both necessary and sufficient for association with the C terminus of LGN, and the entire GoLoco domain appears to be required for the interaction with the N terminus of LGN (Supplemental Figure S4). These data also confirm the specificity of the interaction.

Conceivably, the head-to-tail interaction of LGN could be intermolecular rather than intramolecular and form antiparallel homodimers or filaments. However, it is unlikely that LGN exists predominantly as oligomers in the cell because very little of the endogenous LGN was coprecipitated with YFP-LGN from stably transfected cells (Figure 4C). Therefore, although oligomerization might occur at very high LGN concentrations, it is inefficient under the conditions of our studies, and most of the endogenous LGN likely participates only in intramolecular head-to-tail associations. We provide further evidence in favor of this model below.

LGN Functions as a Conformational Switch

Does this head-to-tail conformation represent a closed state of the protein? To test this hypothesis, we first incubated an N-terminal LGN-GST fusion protein with the C terminus, in the presence of an increasing concentration of NuMA(1818–2001). The GST-LGN was collected onto glutathione-Sepharose beads, and associated proteins were detected by immunoblotting. In the absence of NuMA, the C-terminal LGN domain was specifically coprecipitated with the N-terminal domain. However, increased NuMA binding reduced the association of the C terminus (Figure 4D), consistent with the idea that the NuMA can physically displace the C-terminal domain from its binding site in the N terminus. A similar displacement can be seen using Gαi. When the

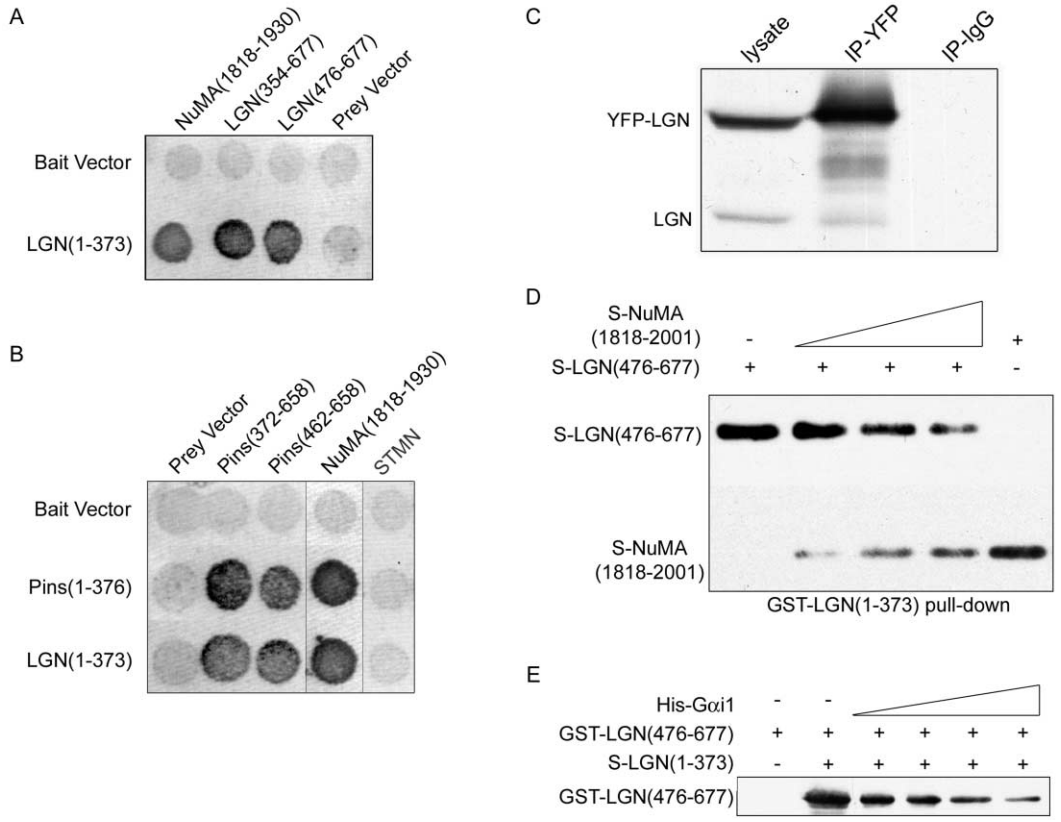

Figure 4. Intramolecular Interactions of LGN

(A and B) Yeast conjugation assays. *S. cerevisiae* HF7C (MATa) transformed with bait vector (pGBT9) or bait vector containing LGN (1–373) (A and B) or Pins (1–376) (B) was conjugated to *S. cerevisiae* W303 (MATα) transformed with empty prey vector (VP16) or prey vectors containing NuMA (1818–1930) (A and B) or LGN C-terminal domain (A) or Pins C-terminal domain (B). Growth of diploids is shown after replica plating onto selective medium ($Leu^-/Trp^-/His^-$ plus 10 mM 3-amino-1,2,4-triazole).

(C) Intermolecular interaction of LGN is not efficient in vivo. Cell lysates from stable YFP-LGN-expressing MDCK cells were immunoprecipitated with anti-GFP antibodies and protein A Sepharose beads. Bound proteins were separated by SDS-PAGE and blotted using anti-LGN antibodies.

(D) NuMA competes with the binding of the LGN N terminus to its C terminus. Equal amounts (200 nM) of GST-LGN (1–373) were loaded on glutathione-Sepharose beads and incubated with 200 nM of S-tagged LGN (476–677) in the absence (lane 1) or presence of 50–200 nM S-tagged NuMA (1818–2001) (lanes 2–4). After washing, bound proteins were separated by SDS-PAGE and blotted using HRP-conjugated S protein.

(E) Gαi1 competes with binding of the LGN C terminus to its N-terminal domain. Equal amounts (200 nM) of S-tagged LGN (1–373) were bound to S-agarose and incubated with 200 nM of GST-LGN (476–677) in the absence (lane 2) or presence of 100–400 nM His-Gαi1 (lanes 3–6). After washing, bound proteins were separated by SDS-PAGE and blotted using anti-GST antibody. Empty beads were also used (lane 1) as a control for nonspecific binding.

C terminus was incubated with the N terminus of LGN in the presence of increasing concentrations of Gαi, the LGN-LGN association was reduced proportionately (Figure 4E).

As a more rigorous test of the conformational switch hypothesis, we developed a LGN biosensor so as to observe changes in the separation of the N and C termini of LGN by fluorescence resonance energy transfer (FRET). Vectors were created to express fusions of YFP-LGN-CFP. If CFP and YFP are in sufficiently close proximity, excitation of CFP can stimulate emission from the YFP fluorophore (Miyawaki, 2003). We tested full-length LGN and a variety of deletion mutants, of which the most effective was LGN(1–610), which lacks the fourth GoLoco motif but appears to be fully functional in binding Gαi and NuMA (Figure 5A and Supplemental Figures S5A and S5B) and which localizes appropriately in mitotic cells (data not shown). This construct, LGN-FRET, exhibits efficient energy transfer in vitro (Figure 5B). The origin of the YFP emission was confirmed by proteinase K treatment, which does not destroy the CFP or YFP but separates the two by cleaving LGN, with the consequent loss of all detectable energy transfer (Figure 5B and Supplemental Figure S5B). Addition of a saturating concentration of either Gαi or a NuMA fragment each produced a similar drop in FRET intensity, consistent with a conformational switch that pushes the YFP and CFP further apart (Figures 5A and 5B). Interestingly, a combination of Gαi plus the NuMA produced a further drop in FRET, suggesting that the binding of either one protein to LGN induces a partially open state, while binding of both induces a fully open state (Figures 5A and 5B).

In principle, similar results might arise if the LGN existed as a head-to-tail dimer that could be dissociated by Gαi or NuMA binding, in the absence of a conformational change. However, serial dilutions of the LGN-FRET bio-

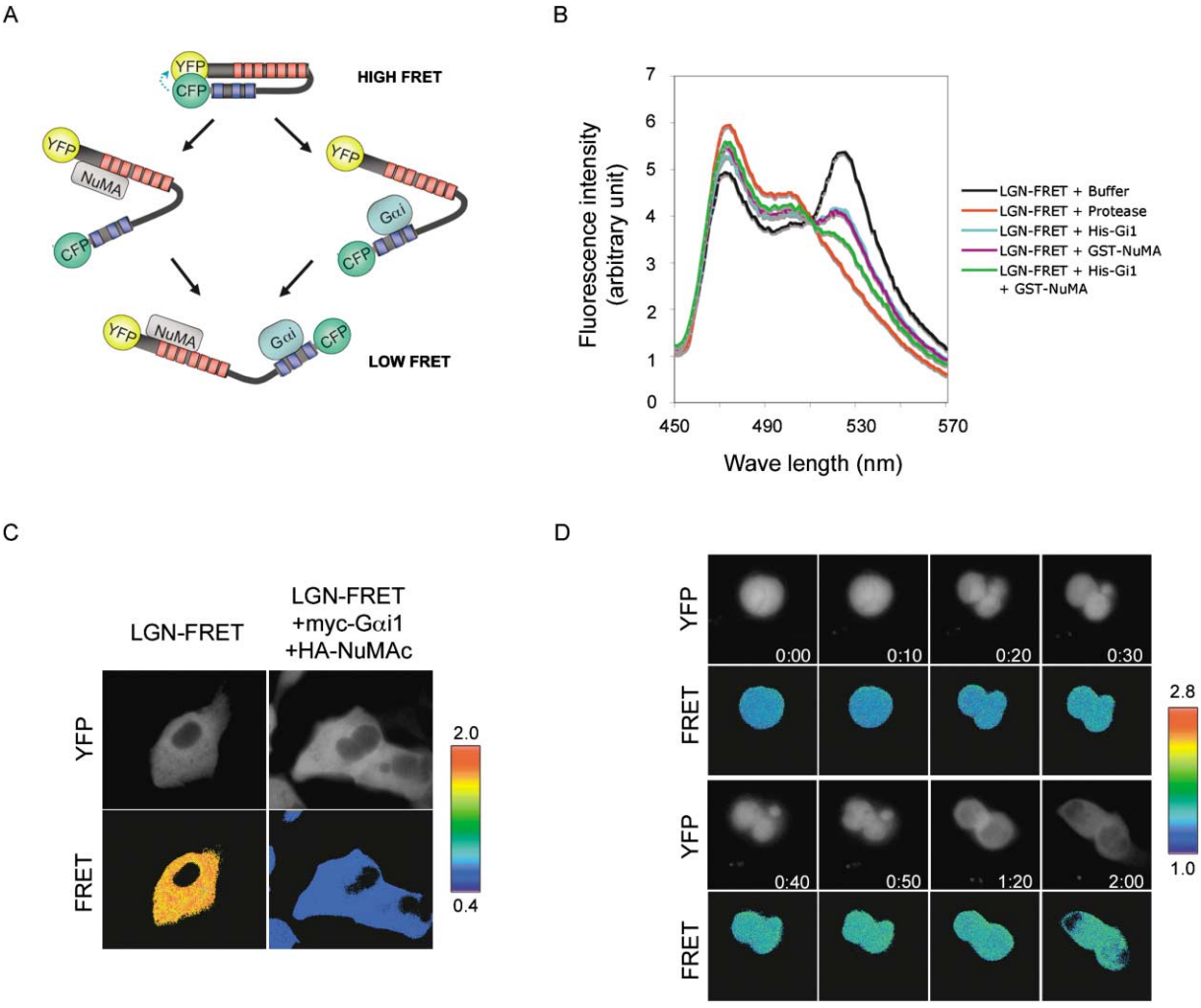

Figure 5. LGN Functions as a Conformational Switch, Responding to NuMA and Gαi Binding

(A) Schematic diagram of LGN-FRET probe and the predicted conformational changes of the probe after binding to NuMA and/or Gαi. TPR motifs (red squares) and GoLoco motifs (blue squares) are indicated. (B) Emission spectra of LGN-FRET (1–610) expressed in COS-7 cells at an excitation wavelength of 433 nm. GST-NuMA (1818–1985) and/or GDP-loaded His-Gαi1 were added (30 μg each) to the cell lysates and incubated at 4°C for 20 min before analysis. For protease digestion, 100 μg/ml proteinase K was added to the cell lysate and incubated at 37°C for 10 min. (C) MDCK II cells were transfected with pKLGN-FRET (1–610) alone (left panel) or cotransfected with pKH3-NuMAcΔNLS and pKmyc-Gαi1 (right panel). Live cell images were obtained with identical exposure times (200 ms) for CFP excitation-CFP emission (data not shown), CFP excitation-YFP emission (data not shown), and YFP excitation-YFP emission (upper panel). The ratio images of CFP excitation-YFP emission/CFP excitation-CFP emission (lower panel) were used to represent FRET efficiency. (D) Time-lapse analysis of LGN-FRET (1–610) probe during and after mitosis. MDCK cells were transfected with pKLGN-FRET (1–610). Transfected mitotic cells were identified by phase contrast and the localization of LGN-FRET. Live cell images were obtained every 10 min as in (C). The ratio image of YFP/CFP (colored images) was used to represent FRET efficiency. The high and low limits of the ratio range are shown at the right of the images in (C) and (D).

sensor over an 80-fold range did not alter the CFP/YFP emission ratio, arguing against the existence of a dissociable LGN dimer (Supplemental Figure S5C).

We next transfected MDCK cells with either LGN-FRET alone or together with vectors to express myc-Gαi and HA3-NuMAc and collected fluorescence images of the cells. The cytoplasmic FRET signals derived from YFP/CFP ratio images were consistently higher ($p < 0.0001$) in those cells that expressed LGN-FRET alone (YFP/CFP ratio $= 1.957 \pm 0.041$, $n = 20$) than in cells coexpressing Gαi and NuMA (YFP/CFP ratio $= 0.796 \pm 0.126$, $n = 20$), consistent with our in vitro results (Figure 5C). The validity of the in vivo FRET signals produced by LGN-FRET was confirmed by showing a significant increase in CFP intensity after photobleaching the YFP (Yoshizaki et al., 2003). From these data, the efficiency of our LGN-FRET probe in vivo was calculated to be 28% ± 4.6% ($n = 10$; see Experimental Procedures).

During interphase, NuMA is confined to the nucleus, so we would expect cytoplasmic LGN to be in the closed state. Therefore, LGN-FRET should display a higher YFP/CFP ratio during intephase, when the nuclear and cytoplasmic components are separated, than in mitosis, when they are mixed. To test this idea, we made movies of LGN-FRET during and after mitosis, in transfected MDCK cells. To avoid photobleaching, the cells were

imaged with low light intensities and 4 × 4 binning on the CCD camera. Under these conditions, the resolution is too low to detect cortical or spindle localization. Nonetheless, we were able to observe a reproducible increase in FRET intensity as the cells exited mitosis (Figure 5D). The FRET signal of mitotic cells (YFP/CFP ratio = 1.674 ± 0.083, n = 20) was consistently lower ($p < 0.0001$) than that of nearby interphase cells (YFP/CFP ratio = 1.957 ± 0.041, n = 20), the signals from which remained constant during the course of the time-lapse imaging (Supplemental Figure S5D).

Taken together, these data confirm that LGN can function as a conformational switch, in which Gαi and NuMA govern the transition between open and closed states, such that the LGN is open in mitosis and closed during interphase.

Allosteric Regulation of NuMA and Gαi Binding to LGN

A key feature of the conformational switch model is that NuMA can increase the affinity of full-length LGN for Gαi and vice versa. LGN is subject to extensive proteolysis when expressed in bacteria. However, we could select for full-length protein by attaching a hexa-His tag to the C terminus and using the interaction with NuMA to capture protein that also contains the N terminus. When we incubated the LGN-His6 with S-tagged NuMA(1818–2001) at concentrations below the estimated equilibrium dissociation constant, this protein was able to bind to the NuMA-coated beads, though only with low efficiency (Figure 6A). Addition of Gαi significantly increased the association of LGN-His6 with S-NuMA(1818–2001).

To test this model in a cellular context, we expressed a C-terminal fragment of NuMA that lacks the nuclear localization signal (NuMA-CT-ΔNLS) but which can bind to LGN. We predicted that this fragment would switch endogenous LGN to the high-affinity state and permit it to associate with the cell cortex even in interphase cells. As shown in Figure 6B, this prediction is correct. Cells that expressed the NuMA fragment showed a significant accumulation of LGN at the plasma membrane in interphase cells. Also consistent with our model, the NuMA fragment, when expressed at relatively low levels, partially colocalized at the plasma membrane with the LGN.

Finally, when a siRNA was directed against NuMA, LGN was absent from the cortex of mitotic cells (Figure 6C). Note that, in HeLa cells, there appears to be a substantial increase in cytoplasmic LGN during mitosis, consistent with the immunoblot data (Figure 1A), and the cortical LGN is concentrated within the regions of the cell poles. We also observed that knockdown of NuMA causes a similar chromosome missegregation phenotype to that caused by the knockdown of LGN (Figure 6C). Together, these data confirm that LGN and NuMA localization to the cell cortex is a codependent phenomenon that also requires cortical Gα.

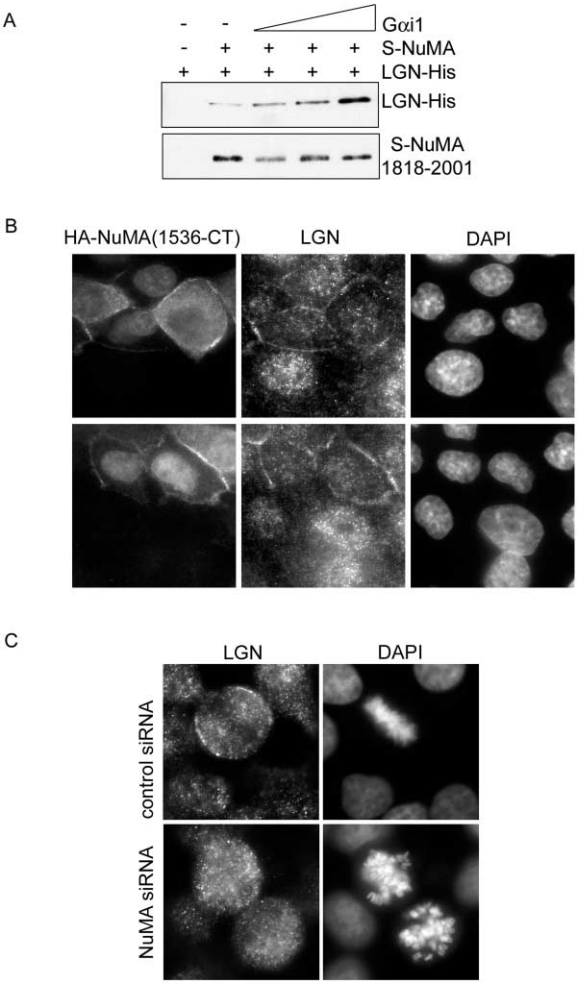

Figure 6. Allosteric Interactions of Gαi1 and NuMA with LGN

(A) Gαi1 increases the binding of NuMA to full-length LGN in vitro. S-tagged NuMA (1818–2001) (20 nM) was loaded on S-agarose beads and incubated with 20 nM of LGN-His6 in the absence (lane 2) or presence of increasing amounts of His-Gαi1 (lanes 3–5). Bound proteins were separated by SDS-PAGE and blotted using anti-His6 antibody.

(B) Overexpression of HA-NuMA-CT-ΔNLS induces the cortical localization of LGN in interphase cells. MDCK cells were transfected with pKH3-NuMA-CT-ΔNLS and stained with monoclonal anti-HA and polyclonal anti-LGN antibodies. DNA was stained with DAPI.

(C) Knockdown of NuMA leads to the dislocalization of LGN from the cell cortex and the spindle poles. HeLa cells were transfected with control siRNA (upper panel) or NuMA siRNA (lower panel). After transfection (72 hr), cells were fixed and stained for LGN. DNA was stained with DAPI.

Gαi and LGN Expression Induce Chromosome Oscillations during Mitosis

The homologs of LGN present in flies and nematodes control spindle orientation and position during asymmetric cell divisions, and this function also requires G proteins (Schaefer et al., 2000, 2001; Yu et al., 2000; Colombo et al., 2003; Gotta et al., 2003; Srinivasan et al., 2003). Therefore, to determine if LGN and Gαi perform a related function in mammalian cells, we examined cells that overexpress LGN or Gαi during mitosis, by time-lapse fluorescence microscopy. We used the inducible cell line that expresses YFP-LGN under the control of the Tet repressor and observed the chromosomes using a vital dye (Hoechst 33342). As described above, at relatively low levels of YFP-LGN expression, no defects of chromosome congression or alignment were observed. Remarkably, however, the metaphase chromo-

somes displayed pronounced rocking motions that were never seen in the control cells (Figure 7A and Supplemental Movies S2 and S3). The oscillation was quasiregular with a period of about 24 ± 6 s and an amplitude of about 30° (Figure 7B). (These are probably underestimates, given the time resolution of 6 s). Importantly, this chromosome movement was not observed when doxycycline was present to inhibit the expression of YFP-LGN (Supplemental Table S1), suggesting that the effect is a direct consequence of YFP-LGN expression.

Conceivably, the chromosome motions could be caused by unequal pulling forces exerted by the spindle MTs, in which case the poles would remain static. Alternatively, the mitotic apparatus might behave as a rigid body, and the poles and chromosomes would rock synchronously, due to unequal pulling forces by the aster MTs. To distinguish these two models, we produced two-channel movies of the mitotic cells, imaging the YFP-LGN in the green channel and DNA in the blue channel. YFP-LGN acts as a marker for the spindle poles. Although the resolution in this experiment is necessarily low (to reduce photobleaching), the two spots that correspond to the spindle poles can be seen to rotate with the metaphase plate (Figure 7C and Supplemental Movie S4; note that the cell cortex is not in focus in these images). Thus, the effect is likely a result of unbalanced forces acting on the mitotic apparatus through the aster MTs.

Although swinging was the predominant motion induced by LGN, occasional parallel or forward and backward movements of the metaphase plate along its long axis were also observed, consistent with the idea that aster MT attachment to the cortex is misregulated. Importantly, however, the motions did not occur out of the plane of the monolayer, suggesting that LGN does not randomize aster attachment sites over the entire cell surface.

The rocking motion induced by YFP-LGN could, in principle, result from transient changes in attachment of the aster MTs to the spindle poles or from changes in attachment to the cell cortex. To try and distinguish these possibilities, we monitored cell lines that express low levels of the isolated N- or C-terminal halves of LGN, fused to YFP. However, neither the N terminus, which localizes to the spindle poles, nor the C terminus, which localizes to the cortex in mitosis, had any effect on orientation of the metaphase plate (Supplemental Table S1). Therefore, functions provided by both ends of the proteins are needed to induce chromosome oscillations.

If the induction of metaphase oscillations is caused by increased LGN recruitment to the cell cortex during mitosis, then an increase in Gαi at the plasma membrane should produce the same phenotype as expression of YFP-LGN. Indeed, we observed rotations of the metaphase chromosomes in Gαi-YFP cells that were indistinguishable from the motion seen in the YFP-LGN cells (Supplemental Table S1 and Supplemental Movie S5). The same phenotype was observed in cells transfected with untagged Gαi (Supplemental Table S1). The specificity of the effect was highlighted by the fact that no oscillations were produced by Gαs, a G protein that does not interact with GoLoco motifs (Natochin et al., 2001) (Supplemental Table S1). Importantly, induction of spindle oscillations requires that the Gαi be at the plasma membrane. Expression of RFP-Gαi, which cannot be myristoylated and is mistargeted to the cytoplasm, did not induce any metaphase oscillations (Supplemental Table S1). The RFP-Gαi also inhibited the oscillations caused by YFP-LGN, confirming that the phenotype specifically requires LGN at the cell cortex (Supplemental Table S1).

Finally, it has been proposed that during the asymmetric cell divisions of *Drosophila* neuroblasts and the *C. elegans* zygote, Gα functions in a receptor-independent signaling pathway downstream of the Pins protein (Schaefer et al., 2001; Srinivasan et al., 2003; Yu et al., 2000). One possibility is that the binding of Pins or GPR-1/2 to Gα releases Gβγ, and Gβγ then regulates the position of the mitotic spindle. However, according to this model, one would expect the overexpression of Gα to inhibit spindle oscillations, which is opposite to the phenotype we observed. To further test whether Gβγ might be required for YFP-LGN-induced spindle rocking motion, we expressed in YFP-LGN cells an RFP-tagged C-terminal fragment of the G protein receptor kinase 2 (GRK2), which can bind to and inhibit Gβγ function (Koch et al., 1993). Expression of the GRK2 C terminus did not inhibit YFP-LGN-induced chromosome movement (Supplemental Table S1), suggesting that Gβγ is probably not involved in this process.

Cortical NuMA and Microtubule Dynamics Regulate Chromosome Oscillation

We used the ΔNLS NuMA C-terminal fragment (NuMA-CT-ΔNLS) to test whether the induction of spindle oscillations requires the association of LGN with NuMA. This fragment will switch LGN to the open state and force it to the cell cortex but will also competitively inhibit the binding of endogenous NuMA to LGN. When transfected into YFP-LGN cells, expression of the NuMA fragment potently inhibited the oscillatory motion (Supplemental Table S1), arguing that endogenous NuMA participates with LGN and Gαi in generating the oscillatory motion of the mitotic apparatus.

Finally, we asked whether the induction of spindle rocking is linked to a change in microtubule dynamics. Low concentrations of nocodazole are known to reduce MT dynamic turnover without causing MT disassembly (Vasquez et al., 1997). We therefore incubated YFP-LGN cells with 10 nM nocodazole and recorded cells that were entering mitosis. This level of nocodazole had no detectable effect on the organization of the bipolar spindles and did not block cells from entering anaphase, but it inhibited spindle rocking (Supplemental Table S1). This result indicates that MT dynamic instability is required to mediate the effects of the NuMA-LGN-Gα complex during mitosis.

Discussion

An important question in developmental biology is how the orientation of mitosis is established. Genetic studies in flies and nematodes have identified a family of related proteins (Pins) that interact with Gα subunits and are essential for the orientation of mitotic spindles in several cell types (Gotta et al., 2003; Schaefer et al., 2000; Srinivasan et al., 2003; Yu et al., 2000). The mammalian homo-

A

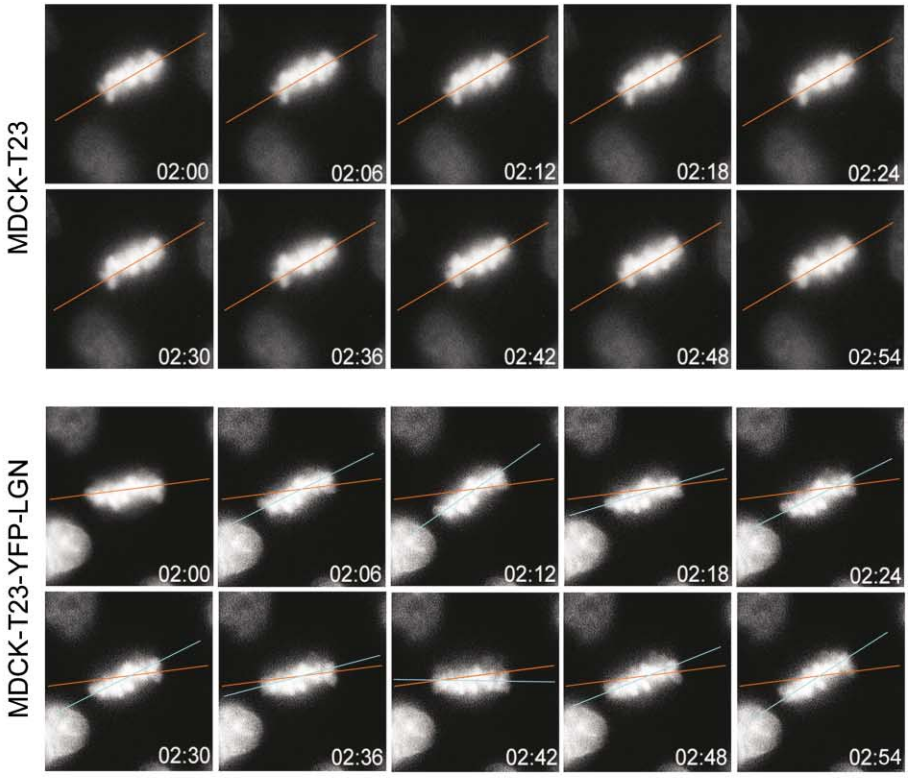
MDCK-T23
02:00
02:06
02:12
02:18
02:24
02:30
02:36
02:42
02:48
02:54
MDCK-T23-YFP-LGN
02:00
02:06
02:12
02:18
02:24
02:30
02:36
02:42
02:48
02:54

B

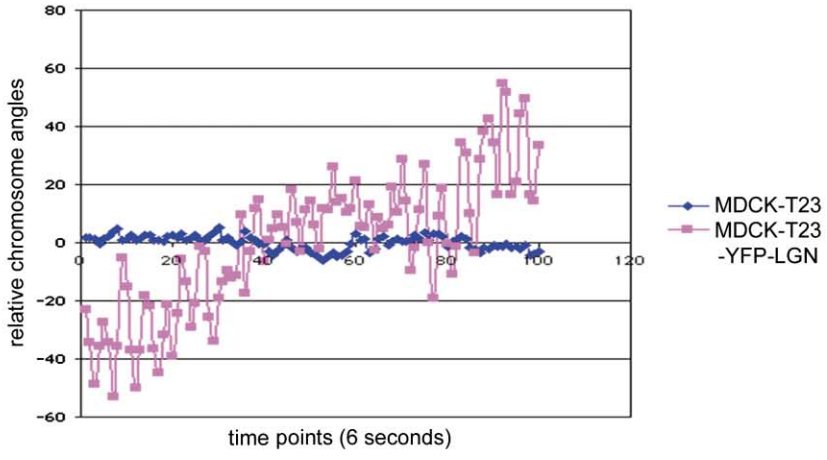
relative chromosome angles
80
60
40
20
0
-20
-40
-60
0
20
40
60
80
100
120
time points (6 seconds)
MDCK-T23
MDCK-T23
-YFP-LGN

C

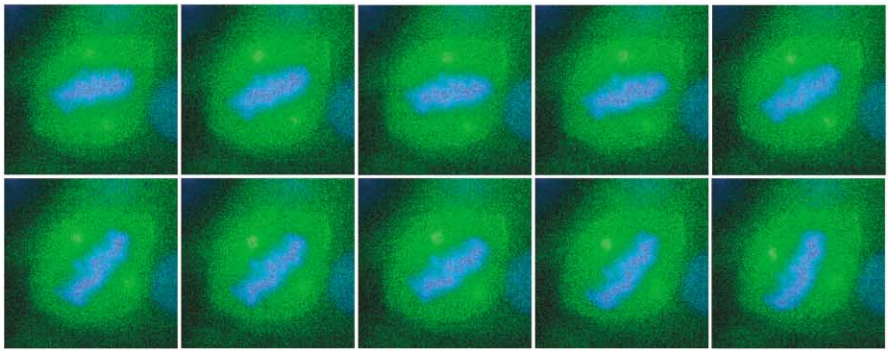

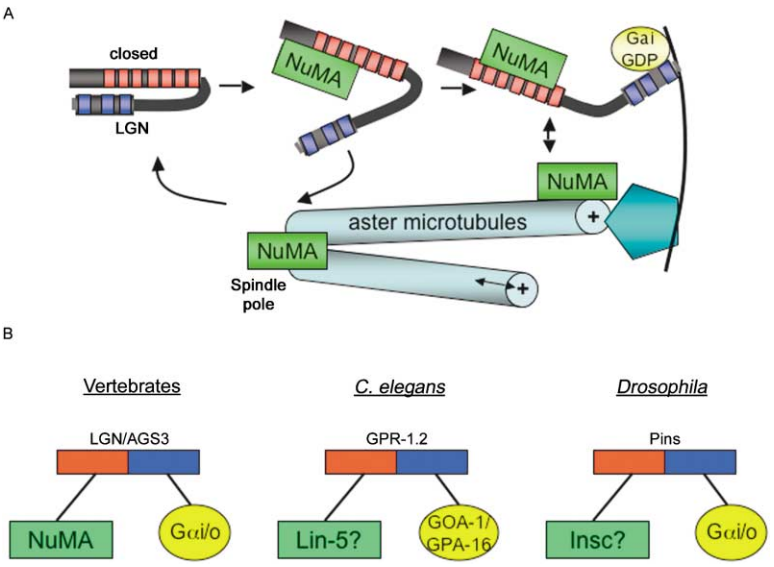

Figure 8. A Model for the Regulation and Function of LGN in Aster Microtubule Attachment

(A) LGN is shown in the closed state in interphase cells, which has a low affinity for Gα. At prophase, as the nuclear envelope is broken down, NuMA is released and binds to LGN, switching it to a partially open state, which has a higher affinity for Gαi:GDP. Gα at the plasma membrane recruits the LGN/NuMA complex. We speculate that, at the membrane, NuMA might be released and bind to aster microtubules, regulating their attachment to dynein or to a cortical attachment factor. Some NuMA/LGN is also targeted to the spindle poles. TPR motifs (red squares) and GoLoco motifs (blue squares) are indicated.

(B) The LGN switch mechanism might be conserved through evolution. A similar ternary complex is proposed to form between the *C. elegans* and *Drosophila* homologs of Pins, Gα, and a third protein.

log of Pins, LGN, also binds to G proteins, but, in addition, it interacts with NuMA, a nuclear protein that is required for spindle organization during mitosis. At the onset of mitosis, when the nuclear envelope breaks down, NuMA can associate with the N-terminal region of LGN, triggering release of the C terminus, so that the LGN switches to a partially open state (Figure 8A). Much of the LGN/NuMA complex associates with the spindle poles, but some can bind with high affinity to Gαi:GDP at the cell cortex to form a ternary complex. To test this model, we developed a FRET biosensor. Our results using LGN-FRET suggest that, in the ternary Gα/LGN/NuMA complex, LGN is in a fully open conformation. We also found that elevating the expression of either LGN or Gαi induces a pronounced rocking motion in the mitotic apparatus of epithelial MDCK cells in culture. This oscillatory motion is similar to motions that have been observed in the embryonic neuroepithelium of the rat cerebral cortex (Adams, 1996). It is also reminiscent of motions observed in the *C. elegans* zygote during anaphase prior to the first asymmetric cell division (Schneider and Bowerman, 2003).

We propose that the ternary NuMA/LGN/Gαi complex perturbs MT cortical attachment, causing transient changes in the pulling forces by the aster MTs on the spindle poles (Figure 8A). Unbalanced pulling forces will produce a torque necessary for rotation of the mitotic apparatus. It remains unclear how the LGN complex alters MT attachment to the cell cortex, but the LGN complex might either increase dynamic instability or modulate the binding of attachment proteins to the plus ends, such as dynein/dynactin. Relevant to this point, NuMA has been previously shown to form a complex with dynein/dynactin in frog egg extracts (Merdes et al., 1996). Gαi itself might also regulate MT dynamics through a direct interaction with tubulin (Willard et al., 2004).

A key observation is that, although the C-terminal NuMA fragment facilitates cortical association of LGN, it also blocks spindle oscillations. This indicates that the oscillations are not simply a consequence of the recruitment of LGN in its open state to the cell cortex but that full-length, endogenous NuMA participates in the process. A second important finding in this regard is that the expression of the isolated N terminus of LGN (which binds NuMA) or the C terminus (which binds Gαi) can each block the recruitment of endogenous NuMA to the cortex of mitotic cells, and neither fragment can induce spindle oscillations. These results show that both the binding of LGN to NuMA and its recruitment to the cortex by Gαi are essential steps in the process. We suggest that LGN is normally the limiting component for cortical localization of the complex and that increased expression of LGN induces spindle oscillations by increasing the amount of NuMA at the cortex. Increased expression of Gαi will induce oscillations by increasing the fraction of endogenous LGN recruited to the cortex.

NuMA stabilizes and can bind to MTs, but it cannot do so when associated with LGN (Du et al., 2002). Conceivably, the ternary LGN complex at the cell cortex is

Figure 7. Expression of YFP-LGN Destabilizes Metaphase Chromosome and Spindle Orientation

(A) Representative fluorescence images taken from a time-lapse sequence showing the motion of Hoechst-stained chromosomes in control (upper two panels) and YFP-LGN-expressing (lower two panels) MDCK T23 cells. Time points are indicated at the lower corner of each image as minutes:seconds. To show the movements of the metaphase plate, the position of the long axis of the plate in the first image was marked by red lines and subsequent positions of the axis marked with light blue lines.

(B) Quantification of chromosome movement of a control (blue) and a YFP-LGN-expressing (red) MDCK T23 cell. Time-lapse images of Hoechst-stained chromosomes were recorded as in (A). The relative angles of the long axis of the chromosome in each frame were measured using Image J software and plotted against time.

(C) Selected continuous frames from a two-channel fluorescence time-lapse recording (6 s per frame) of a YFP-LGN (green) cell also stained with Hoechst 33342 to visualize DNA (blue).

dynamic, such that NuMA is transiently released and can bind MTs, then is either recaptured by LGN or shuttled by dynein down the asters to the spindle pole.

Previous work on asymmetric cell divisions in *Drosophila* and *C. elegans* has led to the proposal that Pins proteins activate G protein signaling in a receptor-independent manner by competing with free $\beta\gamma$ subunits for binding to Gα-GDP (Schaefer et al., 2001; Srinivasan et al., 2003). The $\beta\gamma$ subunits might then generate a signal downstream of Pins that would regulate spindle orientation, or, alternatively, the Pins/Gα-GDP complex might itself generate a downstream signal or be activated to generate Gα-GTP (Willard et al., 2004). Our data do not support the first possibility but are compatible with the second. First, the $\beta\gamma$ signaling model predicts that the overexpression of Gα would reduce spindle oscillations by providing a sink for $\beta\gamma$ subunits, but we observed the opposite effect—Gα expression induced rocking motions of the mitotic apparatus. Second, the $\beta\gamma$ model predicts that the expression of the isolated C terminus of LGN, which contains the GoLoco motifs, would sequester Gα and promote spindle oscillations, but we never observed this phenotype in cell lines that express the LGN C terminus. Finally, expression of the GRK2 C terminus, which can bind $\beta\gamma$ subunits and inhibit their signaling function, had no inhibitory effect on spindle oscillations in the YFP-LGN cell line. The idea that the Pins/Gα-GDP complex generates Gα-GTP, which then signals to the aster MTs, is inconsistent with our observation that the active mutant Gαi(Q204L) does not induce spindle oscillations.

Our results are, however, consistent with a model in which Gαi acts as a targeting factor for Pins rather than as a classical downstream signaling factor. In mammalian cells, the Pins protein is switched to its Gα binding state by NuMA, a protein previously implicated only in spindle pole organization. The cortical localization of NuMA has not been reported previously. Intriguingly, however, a single point mutation in threonine residue 2040 of NuMA causes a dramatic shift in location from the mitotic spindle to the plasma membrane (Compton and Luo, 1995). This residue lies outside of the LGN and MT binding domains in NuMA, so the mutation probably does not directly alter the binding affinity of NuMA for LGN. However, the site is a predicted target for the cell cycle kinase p34cdc2, raising the possibility that the interaction of NuMA and LGN is modulated by phosphorylation. Our observations that mitotic HeLa cells depleted of LGN lack cortical NuMA and that gene silencing of NuMA inhibits the cortical localization of LGN strongly support the idea that this codependent recruitment is a physiologically relevant function of NuMA

Is this function of LGN conserved? Although we do not yet know if the nematode Pins homologs GPR-1,2 function as switches, the N and C termini of the *Drosophila* Pins can associate with one another, suggesting that the conformational switch between open and closed states might be intrinsic to all members of the Pins family. This observation is also consistent with previous data that full-length Pins binds to Gα more weakly than does the isolated C-terminal domain (Schaefer et al., 2001). Remarkably, *Drosophila* Pins can bind to the mammalian NuMA, which implies that the switching mechanism might be very similar throughout the metazoa. However, NuMA is vertebrate-specific, so different proteins presumably act as functional homologs for this protein in other organisms. For example, in *Drosophila* neuroblasts, Insc might be the factor that switches Pins to the open state and facilitates binding to Gα (Schaefer et al., 2000; Yu et al., 2000), and, in *C. elegans*, we speculate that Lin-5 might behave as a NuMA homolog in this context (Figure 8B). Like NuMA, Lin-5 has a large coiled-coil domain, and it binds to GPR-1,2, though the proteins are otherwise dissimilar (Srinivasan et al., 2003).

The next key advance will be to identify the cortical attachment factors for astral MTs that are directly regulated by the Pins/NuMA/Gα complex. The stable cell lines expressing YFP-LGN provide a useful model system for studying the regulation of spindle orientation and cortical attachment by astral MTs in mammalian cells, and the LGN-FRET biosensor provides a tool to observe conformational changes in this protein during the cell cycle.

Experimental Procedures

Cell Lines and Antibodies

HeLa cells, MDCK II, MDCK T23, and stable MDCK T23 cells expressing YFP-LGN were maintained in DMEM (GIBCO) supplemented with 10% FCS and antibiotics at 37°C in a humidified 5% CO_2 atmosphere. Stable inducible MDCK cell lines were made as previously described (Du et al., 2001). Briefly, a superenhanced YFP cDNA (also called Venus [Nagai et al., 2002], a gift from Atsushi Miyawaki, RIKEN, Japan) was cloned into pTRE2Hyg (Clontech). LGN (1–677), LGN (1–373), and LGN (358–677) were inserted downstream of and in frame with YFP, respectively. These plasmids were transfected into MDCK T23 cells, which express the tetracycline-repressible transactivator (Barth et al., 1997). Cells were passaged 24 hr posttransfection onto P-150 plates in medium containing 200 μg ml^{-1} hygromycin B and 20 ng ml^{-1} doxycycline. After selection for 7–10 days, surviving colonies were isolated using cloning rings, and the expression of YFP-fusion proteins was assessed by immunofluorescence and Western blotting after removal of doxycycline.

Rabbit polyclonal anti-LGN antibodies were generated using bacterially expressed C-terminal His6 fusions of full-length human LGN protein as the antigen and affinity purified using LGN-His6 coupled to cyanogen bromide-activated Sepharose beads (Sigma). These new antibodies are more specific than those reported previously (Du et al., 2001). The following antibodies were also used: anti-α-tubulin (Sigma), 9E10 anti-myc, 12CA5 anti-HA, anti-GST, anti-His6 (QIAGEN), anti-Ran, and anti-cyclin B1 (BD Biosciences) mouse monoclonals; and anti-NuMA (a gift from Duane A. Compton, Dartmouth Medical School, New Hampshire) and GFP (Molecular Probes) rabbit polyclonal antibodies.

In Vitro Binding Assays

GST-LGN(1–373) and GST-LGN(476–677) were expressed from pGEX vectors in *E. coli* BL21. His6- and S-tagged NuMA(1818–2001), LGN(1–373), and LGN(476–677) were expressed from the pET30a vector in *E. coli* BL21(DE3) (Novagen). His-tagged LGN(1–677) and Gαi1 (a gift from Maurine Linder, Washington University, St. Louis) were expressed from pQE vectors (Qiagen). His-Gαi1 was loaded with GDP in buffer containing 50 mM Tris-Hcl (pH 8.0), 1 mM EDTA, 1 mM DTT, 50 mM ATP, and 30 μM GDP at room temperature for 1 hr. Binding assays were performed using glutathione-Sepharose 4B (Amersham Biosciences) or S protein agarose (Novagen) beads in binding buffer (50 mM HEPES [pH 7.5], 150 mM NaCl, 5 mM $MgCl_2$, 1 mM DTT, and 0.01% Tween-20) as described (Du et al., 2001). After washing, bound proteins were separated by SDS-PAGE and detected by immunoblotting using anti-GST (1:2000), anti-His6 (1:1000), or horseradish peroxidase (HRP)-coupled S protein (Du et al., 2001).

Yeast Conjugation Assay

Yeast conjugation assays were carried out as previously described (Joberty et al., 2000) using yeast strains HF7c (Mat-a) and W303 (Mat-α). The two mating types, transformed with pGBT9 or pVP16 vectors, were mixed and incubated overnight on rich medium plates to allow mating. The following day, colonies were replica plated onto selective medium ($Leu^-/Trp^-/His^-$ plus 10 mM 3-amino-1,2,4-triazole) and incubated at 30°C to allow growth of diploids.

Transfection and Immunoprecipitation

For immunofluorescence microscopy, cells were transfected using either the Effectene reagent kit (Qiagen) or an electroporation device (Amaxa) following the manufacturers' instructions. For immunoprecipitation, COS-7 or HeLa cells were transfected with mammalian expression vectors by calcium phosphate method as previously described. Cells were collected in lysis buffer (25 mM HEPES [pH 7.4], 150 mM NaCl, 0.5% Triton X-100, 0.5 mM EDTA, 5 mM $MgCl_2$, 1 mM DTT, 1 mM PMSF, 10 μg ml^{-1} leupeptin, and 20 μg ml^{-1} aprotinin). Equal amounts of cell lysate were incubated with 2 μg of anti-myc antibody at 4°C for 1 hr. GammaBind-Plus Sepharose beads (Amersham Biosciences), blocked with 5% BSA, were added, and the mixture was incubated for 45 min at 4°C. Immunoprecipitates were washed four times with lysis buffer and separated by SDS-PAGE. Proteins were transferred to nitrocellulose and detected using anti-LGN (1:1000), anti-NuMA (1:2000) or anti-HA (1:500) antibodies.

Immunofluorescence Microscopy

Cells were grown on Lab-Tek Chamber Slides (Nalge Nunce International) and fixed using either 4% paraformaldehyde in PBS or 3% paraformaldehyde/0.5% Triton X-100 in PHEM buffer (60 mM PIPES, 25 mM HEPES, 10 mM EGTA, and 5 mM $MgSO_4$ [pH 6.9]) as indicated. Fixed cells were blocked with 1% BSA/10% FCS in PBS for 1 hr, then incubated for 1 hr with the following primary antibodies: anti-LGN (1:200), anti-NuMA (1:1500), anti-α-tubulin (1:2000), and 12CA5 anti-HA (1:500). Cells were then washed and incubated for 1 hr with the DNA stain DAPI and goat anti-rabbit or anti-mouse secondary antibodies coupled to Alexa 488 or Alexa 594 (Molecular Probes). A SlowFade Light AntiFade kit (Molecular Probes) was used to inhibit photobleaching. Cells were imaged using ×60/1.2 N.A. water-immersion objective or ×100/1.4 N.A. oil objective on a Nikon Eclipse TE 200 inverted microscope. Images were collected using Openlab 3.1 software (Improvision) and processed for publication with Adobe Photoshop. For comparison of fluorescent intensities, regions of interest were marked and measured using Openlab 3.1.

Construction of LGN-FRET Probes and In Vitro Spectrofluorometry

The open reading frames of YFP (aa 1–228) and CFP (aa 1–237) were cloned into the pK vector with BamHI/NotI/EcoRI restriction sites between YFP and CFP to create pKFRET. LGN fragments were then cloned in the NotI site of pKFRET to make pKLGN-FRET vectors. pKLGN-FRET plasmids were transfected into COS-7 cells by the calcium phosphate method. At 36 hr after transfection, cells were collected in lysis buffer (20 mM Tris-HCl [pH 7.5], 100 mM NaCl, 5 mM $MgCl_2$, 0.5% Triton X-100, 1 mM DTT) and clarified by centrifugation. Fluorescence spectra were obtained with a spectrofluorometer (Fluorolog, model FL3-11tau, JOBIN YVON INC.) using an excitation wavelength of 433 nm and 4 nm slits.

Live Cell Time-Lapse Imaging

Cells were grown on Delta T dishes (Bioptechs, Inc) in DMEM supplemented with 10% FCS and antibiotics. For visualizing chromosome movement, the medium was replaced with F10 medium containing 2 μg ml^{-1} of Hoechst 33342 and incubated for 5 min. After several washes, the dish was filled with F10 medium containing 0.3 unit ml^{-1} OxyFluor (Oxyrase, Inc) and sealed with a large coverslip. The dish was then placed in a temperature control system (Bioptechs, Inc) that maintained a temperature of 37°C. Time-lapse sequences were collected on a Nikon Eclipse TE200 microscope using a X100/1.4 N.A. objective, an ORCA CCD camera (Hamamatsu), and Openlab 3.1 software (Improvision). For quantification of chromosome movements, Image J and Micosoft Excel were used. Dual-emission ratio imaging of LGN-FRET was performed as described above, without the addition of Hoechst dye. We used excitation filters S436/10× for CFP and S500/20× for YFP and emission filters S470/30m for CFP and S535/30m for YFP (Chroma Technology Corp.). Cells were illuminated through a 25% ND filter to reduce photobleaching. The exposure time was 0.2 s, and the binning of the CCD camera was 4 × 4. After background subtraction, FRET images were created using the Openlab 3.5 FRET module. FRET values were calculated for 20 cells in each experiment and are presented as the means ± 1 SD. The significance of differences in FRET was evaluated using an unpaired Student's t test. To validate the FRET signals in vivo, photobleaching experiments were performed as described (Yoshizaki et al., 2003). The FRET efficiency was obtained by the following equation: FRET efficiency = 1 − CFP prebleach/CFP postbleach.

Gene Silencing by RNA Interference

RNAi was carried out using synthetic siRNA duplexes in HeLa cells as described previously (Du et al., 2001). The sequences of the regions targeted for siRNA in human LGN and NuMA cDNA have been given elsewhere (Du et al., 2001; Elbashir et al., 2001). Oligonucleotides were purchased from Dharmacon.

Acknowledgments

We thank Maurine Linder (Washington University, MO) for the Gαi-His_6 expression vector; Duane Compton (Dartmouth University, NH) for anti-NuMA antibodies and the NuMA cDNA; Roger Tsien (UCSD) for mRFP1; Atsushi Miyawaki (RIKEN, Japan) for Venus; Doug Bayliss (University of Virginia) for the GRK2 C terminus, Gαi, and Gαi1(Q204L); Mark Rasenick (University of Illinois, Chicago) for Gαs-GFP; Keith Mostov (UCSF) for MDCK T23 cell line; and Juergen Knoblich (IMP, Vienna, Austria) for the Pins cDNAs. We also thank Anne Spang (Tübingen) for valuable comments on the manuscript. This work was supported by grants PO1CA40042 and R01 GM070902 from the National Institutes of Health, DHHS.

Received: April 14, 2004
Revised: August 12, 2004
Accepted: October 8, 2004
Published: November 11, 2004

References

Adams, R.J. (1996). Metaphase spindles rotate in the neuroepithelium of rat cerebral cortex. J. Neurosci. *16*, 7610–7618.

Barth, A.I., Pollack, A.L., Altschuler, Y., Mostov, K.E., and Nelson, W.J. (1997). NH2-terminal deletion of beta-catenin results in stable colocalization of mutant β-catenin with adenomatous polyposis coli protein and altered MDCK cell adhesion. J. Cell Biol. *136*, 693–706.

Cayouette, M., and Raff, M. (2002). Asymmetric segregation of Numb: a mechanism for neural specification from *Drosophila* to mammals. Nat. Neurosci. *5*, 1265–1269.

Colombo, K., Grill, S.W., Kimple, R.J., Willard, F.S., Siderovski, D.P., and Gonczy, P. (2003). Translation of polarity cues into asymmetric spindle positioning in *Caenorhabditis elegans* embryos. Science *300*, 1957–1961.

Compton, D.A. (2000). Spindle assembly in animal cells. Annu. Rev. Biochem. *69*, 95–114.

Compton, D.A., and Luo, C. (1995). Mutation of the predicted p34cdc2 phosphorylation sites in NuMA impair the assembly of the mitotic spindle and block mitosis. J. Cell Sci. *108*, 621–633.

Compton, D.A., Szilak, I., and Cleveland, D.W. (1992). Primary structure of NuMA, an intranuclear protein that defines a novel pathway for segregation of proteins at mitosis. J. Cell Biol. *116*, 1395–1408.

Doe, C.Q., and Bowerman, B. (2001). Asymmetric cell division: fly neuroblast meets worm zygote. Curr. Opin. Cell Biol. *13*, 68–75.

Du, Q., Stukenberg, P.T., and Macara, I.G. (2001). A mammalian Partner of inscuteable binds NuMA and regulates mitotic spindle organization. Nat. Cell Biol. *3*, 1069–1075.

Du, Q., Taylor, L., Compton, D.A., and Macara, I.G. (2002). LGN blocks the ability of NuMA to bind and stabilize microtubules. A

mechanism for mitotic spindle assembly regulation. Curr. Biol. *12*, 1928–1933.

Elbashir, S.M., Harborth, J., Lendeckel, W., Yalcin, A., Weber, K., and Tuschl, T. (2001). Duplexes of 21-nucleotide RNAs mediate RNA interference in cultured mammalian cells. Nature *411*, 494–498.

Gaglio, T., Saredi, A., and Compton, D.A. (1995). NuMA is required for the organization of microtubules into aster-like mitotic arrays. J. Cell Biol. *131*, 693–708.

Gordon, M., Howard, L., and Compton, D. (2001). Chromosome movement in mitosis requires microtubule anchorage at spindle poles. J. Cell Biol. *152*, 425–434.

Gotta, M., and Ahringer, J. (2001). Distinct roles for Gα and Gβγ in regulating spindle position and orientation in *Caenorabditis elegans* embryos. Nat. Cell Biol. *3*, 297–300.

Gotta, M., Dong, Y., Peterson, Y.K., Lanier, S.M., and Ahringer, J. (2003). Asymmetrically distributed *C. elegans* homologs of AGS3/PINS control spindle position in the early embryo. Curr. Biol. *13*, 1029–1037.

Grill, S.W., Gonczy, P., Stelzer, E.H., and Hyman, A.A. (2001). Polarity controls forces governing asymmetric spindle positioning in the *Caenorhabditis elegans* embryo. Nature *409*, 630–633.

Grill, S.W., Howard, J., Schaffer, E., Stelzer, E.H., and Hyman, A.A. (2003). The distribution of active force generators controls mitotic spindle position. Science *301*, 518–521.

Haren, L., and Merdes, A. (2002). Direct binding of NuMA to tubulin is mediated by a novel sequence motif in the tail domain that bundles and stabilizes microtubules. J. Cell Sci. *115*, 1815–1824.

Jan, Y.N., and Jan, L.Y. (2001). Asymmetric cell division in the *Drosophila* nervous system. Nat. Rev. Neurosci. *2*, 772–779.

Joberty, G., Petersen, C., Gao, L., and Macara, I.G. (2000). The cell-polarity protein Par6 links Par3 and atypical protein kinase C to Cdc42. Nat. Cell Biol. *2*, 531–539.

Kaushik, R., Yu, F., Chia, W., Yang, X., and Bahri, S. (2003). Subcellular localization of LGN during mitosis: evidence for its cortical localization in mitotic cell culture systems and its requirement for normal cell cycle progression. Mol. Biol. Cell *14*, 3144–3155.

Koch, W.J., Inglese, J., Stone, W.C., and Lefkowitz, R.J. (1993). The binding site for the β/γ subunits of heterotrimeric G proteins on the β-adrenergic receptor kinase. J. Biol. Chem. *268*, 8256–8260.

Macara, I.G. (2004). Parsing the polarity code. Nat. Rev. Mol. Cell Biol. *5*, 220–231.

Merdes, A., Ramyar, K., Vechio, J.D., and Cleveland, D.W. (1996). A complex of NuMA and cytoplasmic dynein is essential for mitotic spindle assembly. Cell *87*, 447–458.

Miyawaki, A. (2003). Visualization of the spatial and temporal dynamics of intracellular signaling. Dev. Cell *4*, 295–305.

Nagai, T., Ibata, K., Park, E.S., Kubota, M., Mikoshiba, K., and Miyawaki, A. (2002). A variant of yellow fluorescent protein with fast and efficient maturation for cell-biological applications. Nat. Biotechnol. *20*, 87–90.

Natochin, M., Gasimov, K.G., and Artemyev, N.O. (2001). Inhibition of GDP/GTP exchange on G alpha subunits by proteins containing G-protein regulatory motifs. Biochemistry *40*, 5322–5328.

Reinsch, S., and Karsenti, E. (1994). Orientation of spindle axis and distribution of plasma membrane proteins during cell division in polarized MDCKII cells. J. Cell Biol. *126*, 1509–1526.

Schaefer, M., Shevchenko, A., and Knöblich, J.A. (2000). A protein complex containing Inscuteable and the Galpha-binding protein Pins orients asymmetric cell divisions in *Drosophila*. Curr. Biol. *10*, 353–362.

Schaefer, M., Petronczki, M., Dorner, D., Forte, M., and Knöblich, J.A. (2001). Heterotrimeric G proteins direct two modes of asymmetric cell division in the *Drosophila* nervous system. Cell *107*, 183–194.

Schneider, S.Q., and Bowerman, B. (2003). Cell polarity and the cytoskeleton in the *Caenorhabditis elegans* zygote. Annu. Rev. Genet. *37*, 221–249.

Srinivasan, D.G., Fisk, R.M., Xu, H., and van den Heuvel, S. (2003). A complex of LIN-5 and GPR proteins regulates G protein signaling and spindle function in *C elegans*. Genes Dev. *17*, 1225–1239.

Vasquez, R.J., Howell, B., Yvon, A.M., Wadsworth, P., and Cassimeris, L. (1997). Nanomolar concentrations of nocodazole alter microtubule dynamic instability in vivo and in vitro. Mol. Biol. Cell *8*, 973–985.

Whitfield, M.L., Sherlock, G., Saldanha, A.J., Murray, J.I., Ball, C.A., Alexander, K.E., Matese, J.C., Perou, C.M., Hurt, M.M., Brown, P.O., and Botstein, D. (2002). Identification of genes periodically expressed in the human cell cycle and their expression in tumors. Mol. Biol. Cell *13*, 1977–2000.

Willard, F.S., Kimple, R.J., and Siderovski, D.P. (2004). Return of the GDI: the GoLoco motif in cell division. Annu. Rev. Biochem. *73*, 925–951.

Yoshizaki, H., Ohba, Y., Kurokawa, K., Itoh, R.E., Nakamura, T., Mochizuki, N., Nagashima, K., and Matsuda, M. (2003). Activity of Rho-family GTPases during cell division as visualized with FRET-based probes. J. Cell Biol. *162*, 223–232.

Yu, F., Morin, X., Cai, Y., Yang, X., and Chia, W. (2000). Analysis of Partner of Inscuteable, a novel player of *Drosophila* asymmetric divisions, reveals two distinct steps in Inscuteable apical localization. Cell *100*, 399–409.

Yu, F., Morin, X., Kaushik, R., Bahri, S., Yang, X., and Chia, W. (2003). A mouse homologue of *Drosophila* pins can asymmetrically localize and substitute for pins function in *Drosophila* neuroblasts. J. Cell Sci. *116*, 887–896.